Scattering of Alpha Particles by Oxygen. II. Bombarding Energy Range 10 to 19 MeV*

M. K. Mehta†, W. E. Hunt,‡ and R. H. Davis

Department of Physics, Florida State University, Tallahassee, Florida

(Received 13 October 1966)

The $O^{16}(\alpha,\alpha)O^{16}$ and $O^{16}(\alpha,\alpha'\gamma)O^{16}$ reactions have been studied in the bombarding energy range from 10.0 to 19.0 MeV. Elastic-scattering differential cross sections were measured at eight angles as a function of energy, and a total of thirty-five levels in the compound nucleus Ne^{20} have been observed in the excitation curves. Angular distributions of the elastically scattered α particles have been measured at seven energies and each shows a strong dependence of the differential cross section on angle. These were analyzed in terms of the Ackhiezer-Pomeranchuk-Blair-McIntyre (APBM) model and the nuclear optical model. Good theoretical fits to the experimental data were obtained only when contributions from resonances were included explicitly in the APBM-model calculations. Excitation curves for the γ rays emitted from nuclei excited in inelastic-scattering events have been measured, and the Ne^{20} energy levels found in the γ-ray excitation curves confirm most of the levels found in the elastic-scattering experiment. Thin- and thick-target angular distributions for the 6.13-MeV γ rays were measured at 15 energies. Thick-target γ-ray angular distributions which average over many resonances could not be simply interpreted in terms of broad levels in Ne^{20}. Twenty spin-and-parity assignments to states in Ne^{20} have been made in the analysis of the elastic- and inelastic-scattering data, and of these, 14 are tentative. The levels in Ne^{20} observed here have broader widths, larger spacings, and greater spins than the majority of those reported in the literature for the same excitation energy range. These differences are discussed and a possible explanation is offered. The incorporation of several of the levels found in this work in Ne^{20} rotational bands has been included in Paper I.

I. INTRODUCTION

IN Paper I[1] (the preceding paper), the work of Cameron[2] and McDermott *et al.*[3] is extended through the α-particle bombarding energy 6–10 MeV. This study of the scattering of α particles by O^{16} is a continuation of Paper I with the distinction that here more than one channel is open. The bombarding energy 10–19 MeV (12.72–19.93-MeV excitation in Ne^{20}) overlaps the range of Paper I and includes the bombarding energy of the experiment performed by Corelli *et al.*[4] at 18.3 MeV. An extreme back-angle excitation curve for beam energies 14.0–22.7 MeV and several angular distributions between 21.2 and 22.7 MeV have been measured by Jodogne *et al.*[5] Blatchley and Bent[6] measured angular distributions of the elastically and inelastically scattered α particles at 22.5 MeV. Beyond this range are the investigations of Aguilar *et al.*[7] at 38

MeV, Yavin and Farwell[8] at 40 MeV, and Harvery *et al.*[9] at 65 MeV.

Two sets of experiments have been performed and the paper is divided accordingly. Section II contains the results of the elastic-scattering experiments and their analysis. Excitation functions for the elastic scattering of α particles from O^{16} have been measured at eight angles in a bombarding-energy range 10–19 MeV. Angular distributions have been obtained at seven energies, and at 18.3 MeV, the distribution is in good agreement with the distribution measured by Corelli *et al.*[4]

In Sec. III, the measurements of γ rays produced by the inelastic scattering of α particles by O^{16} are discussed. The spin and parity of the first excited state of O^{16} at 6.06 MeV are the same as those of the ground state 0^+, and this decay transition was not observed. Excitation functions of the 6.13-MeV γ rays from the second excited state of O^{16} and of the unresolved 6.92- and 7.12-MeV γ rays from the third and the fourth excited states have been measured at zero degrees over the same energy range as that in the elastic-scattering experiment. Angular distributions for the 6.13-MeV γ rays were measured at a number of energies.

The existence of 35 levels in Ne^{20} with excitation energies between 12.72 and 19.93 MeV is inferred from the experimental results. A total of 20 spin and parity assignments are given, 6 of which are firm and 14 tentative. Initially, the behavior of the elastic-scattering excitation curves at selected angles was used to make

[1] W. E. Hunt, M. K. Mehta, and R. H. Davis, preceding paper, Phys. Rev. **160**, 782 (1967).

[2] J. R. Cameron, Phys. Rev. **90**, 839 (1953).

[3] L. C. McDermott, K. W. Jones, H. Smotrich, and R. E. Benenson, Phys. Rev. **118**, 175 (1960).

[4] J. C. Corelli, E. Bleuler, and D. J. Tendem, Phys. Rev. **116**, 1184 (1959).

[5] J. C. Jodogne, P. C. Macq, and J. Steyaert, Phys. Letters **2**, 325 (1962).

[6] D. E. Blatchley and R. D. Bent, Nucl. Phys. **61**, 641 (1965).

[7] J. Aguilar, W. E. Burcham, J. Catala, J. B. A. England, J. S. C. McKee, and J. Rotblat, Proc. Roy. Soc. (London) **A254**, 395 (1960).

[8] A. I. Yavin and G. W. Farwell, Nucl. Phys. **12**, 1 (1959).

[9] B. G. Harvey, E. J-M. Rivet, A. Springer, J. R. Meriwether, W. B. Jones, J. H. Elliott, and P. Darriulat, Nucl. Phys. **52**, 465 (1964).
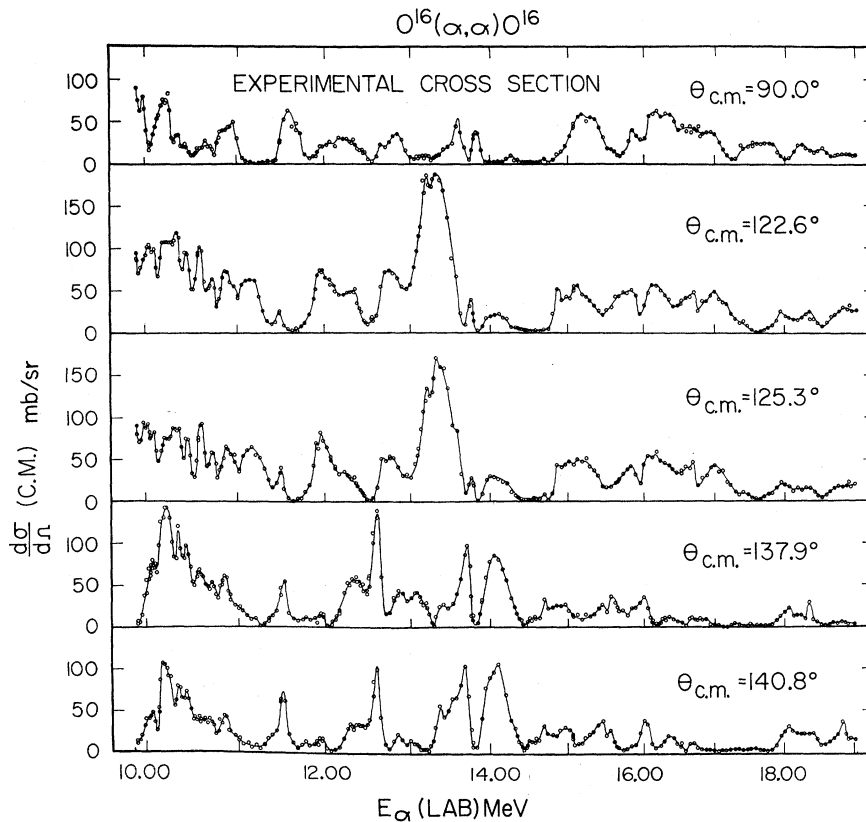
$O^{16}(\alpha,\alpha)O^{16}$

FIG. 1. $O^{16}(\alpha,\alpha)O^{16}$ differential cross sections for laboratory α-particle energies from 10.00 to 19.00 MeV. The center-of-mass observation angles are 90°, 122.6°, 125.3°, 137.9°, and 140.8°.

18 tentative assignments. Five of these were confirmed by analyses of the elastic-scattering angular distribution that also characterized one previously unlabeled level. A study of the angular distributions of the γ rays produced a reconfirmation of one assignment and gave one additional tentative assignment.

Four reactions, (α,α), (α,α'), (α,p), and (α,n) are energetically possible, but only the elastically scattered particles and the γ-ray yield associated with the inelastic scattering were measured in this investigation. This limitation, coupled with the complexity of the structure in the excitation curves, restricted the type of analysis that could be undertaken.

The elastic-scattering angular distributions have been fitted with the Ackhiezer-Pomeranchuk-Blair-McIntyre (APBM) model, originally introduced by Ackhiezer and Pomeranchuk,[10] interpreted for α-particle scattering by Blair,[11] and modified by McIntyre[12] to improve fits to backward-angle data. The inclusion of resonance terms was necessary for good fits. In principle, the optical model with resonance terms can be used to fit the data, but the trial fits without resonance terms showed no advantage at the time.

Assumptions have been made in the γ-ray analysis

[10] A. Ackhiezer and L. Pomerancuk, J. Phys. (USSR) **9**, 471 (1945).
[11] J. S. Blair, Phys. Rev. **95**, 1218 (1954).
[12] J. A. McIntyre, K. H. Wang, and L. C. Becker, Phys. Rev. **117**, 1337 (1960).

which make the calculations tractable, but which also oversimplify the physics. Nonetheless, several useful results have been obtained.

Information about Ne^{20} excited states found in this work is compared in Sec. IV with that previously known. The spacings, widths, and spins of levels observed here are generally larger than those reported in the literature. Some of the differences can be attributed to the general characteristics of α-particle scattering, while other features are more intimately related to the details of the α-particle interaction mechanism.

Several of the levels identified in this work are included in the discussion of rotational bands in Ne^{20} which is given in Paper I.[1]

II. ELASTIC-SCATTERING EXPERIMENT

A. Experimental Technique

The experimental techniques used in the measurement of the elastically scattered α-particle yield are discussed in Paper I.[1] Energies were determined to ± 20 keV. The estimated error in the differential cross sections is $\pm 12\%$, except where the differential cross section is less than 5 mb/sr, and here low counting rates resulted in large statistical errors.

Excitation curves were measured at eight angles by measuring the yield incident upon each detector for a fixed-charge collection as a function of energy in steps
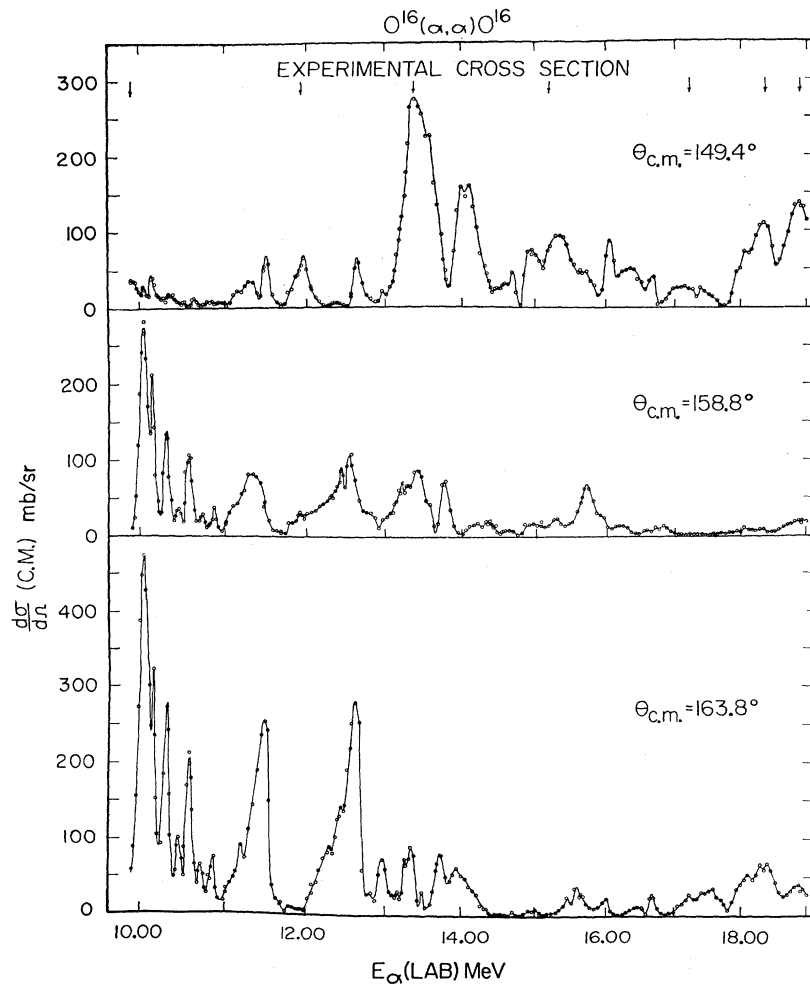
$O^{16}(\alpha,\alpha)O^{16}$

FIG. 2. $O^{16}(\alpha,\alpha)O^{16}$ differential cross sections for laboratory α-particle energies from 10.00 to 19.00 MeV. The center-of-mass observation angles are 149.4°, 158.8°, and 163.8°.

of 50 keV. Smaller energy steps were chosen where necessary. Observation angles were those corresponding to zeros of Legendre polynomials of orders 1 through 8. In the angular-distribution measurements, the yield in each of two rotating counters was measured as a function of angles in steps of 3°. The third rotating counter was used as a fixed monitor.

B. Data

The experimental absolute differential cross section at eight angles as a function of bombarding energy is shown in Figs. 1 and 2. Figures 3 and 4 show the experimental differential cross sections as a function of center-of-mass angles at seven energies. The dots are the experimental points, and the lines are the theoretical fits which are discussed in the following sections. Within experimental errors, the angular distribution at 18.3 MeV is the same as the one measured by Corelli et al.[4]

C. Analysis of the Excitation Curve

The differential cross section for elastic scattering can be expressed in terms of the partial waves and the cor-

responding phase shifts.[13] When only the elastic channel is open and levels do not overlap, the single-level dispersion theory of Wigner and Eisenbud[14,15] is a good approximation. The analysis is complicated when more than one channel is open and when levels are not well separated, which is the case in the present experiment.

Irrespective of the number of channels and the level density, the nuclear-scattering term in the expression for the scattering amplitude for each partial wave involves the Legendre polynomial of corresponding order. Where this term vanishes, the effect of a resonance which is excited by the lth partial wave will also vanish. Since the channel spin is zero, total angular momentum J is equal to the orbital angular momentum l, and the parity of the state will be odd for odd J and even for even J, i.e., only natural-parity energy levels are detected in this experiment. Information about the spin and parity of a number of levels was obtained from an

[13] J. M. Blatt and V. F. Weisskopf, Theoretical Nuclear Physics (John Wiley & Sons, Inc., New York, 1952).
[14] E. P. Wigner and L. Eisenbud, Phys. Rev. 72, 29 (1947).
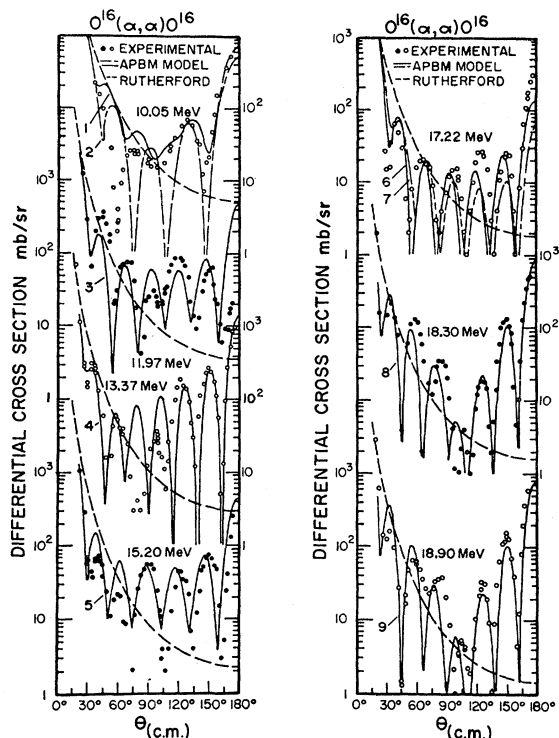[15] A. M. Lane and R. G. Thomas, Rev. Mod. Phys. 30, 257 (1958).

FIG. 3. Experimental and theoretical angular distributions for $O^{16}(\alpha,\alpha)O^{16}$. The dots are experimental values, and the lines are theoretical fits calculated with the APBM model. Parameters used for each of the curves are listed in Table II.

The γ-ray angular-distribution analyses (see Sec. III) provide additional information about the spin and parity assignments shown in Table I. A level observed in the γ-ray experiment at a bombarding energy of 10.39 MeV ($E_x = 13.03$ MeV) is assigned a spin and parity of 4^+ or 5^-, which is in weak support of the tentative 4^+ assignment made to the level at an estimated excitation energy of 13.07 MeV in the elastic-scattering work. A tentative 2^+ assignment is shown for the wide level at excitation energy 17.32 MeV. This is based on the γ-ray angular-distribution measurement at 15.705 MeV ($E_x = 17.29$ MeV).

A large number of levels have been identified in this region of excitation in Ne^{20} by a number of studies[16,17] of reactions induced by proton bombardment of F^{19}. Prior to this publication, the results of this work were compared with those of the $F^{19}+p$ experiments by Jenkin et al.[18] Some of the levels in Table I correspond to these previously observed levels. Not all the levels found in the $F^{19}+p$ experiment may be seen in this ex-

examination of the excitation curves, which were measured at angles corresponding to the zeros of Legendre polynomials of orders 1 through 8. The certainty of such assignments depends upon the magnitudes and isolation of the anomaly in the excitation curves. Where the level density is high, they are subjective and should be considered unambiguous only when confirmed by another method.

Approximately 35 anomalies were found in the excitation curve, and only the more prominent resonances were analyzed in detail. Resonance energies were determined by excitation-curve inspection rather than a phase-shift analysis fit to the excitation curve. Considerably more data is required for a significant phase-shift analysis. As a result, a resonance energy may be ill defined, the maximum error of which is the width of the resonance. Observed widths of most of the resonances were much larger than the energy loss in the target. A value of 4.730 MeV was assumed for the separation energy for an α particle in Ne^{20}.

In Table I, 35 Ne^{20} levels identified in the elastic-scattering experiment are listed along with estimated laboratory widths and the spin-and-parity assignments. Five of the eighteen tentative assignments from excitation curves are confirmed in the angular-distribution analyses. The 6^+ assignment at 15.18-MeV incident energy is based on angular-distribution data only.

FIG. 4. Experimental and theoretical angular distributions for $O^{16}(\alpha,\alpha)O^{16}$. The dots are experimental values, and the lines are theoretical fits calculated with the optical model. Parameters used for each of the curves are listed in Table III.

[16] F. Ajzenberg-Selove and T. Lauritsen, Nucl. Phys. **11**, 1 (1958).

[17] T. Lauritsen and R. Ajzenberg-Selove, in *Nuclear Data Sheets*, compiled by K. Way et al. (Printing and Publishing Office, National Academy of Sciences—National Research Council, Washington, D. C., 1962), Sets 5 and 6.

[18] J. G. Jenkin, L. G. Earwaker, and E. W. Titterton, Nucl. Phys. **44**, 453 (1963).

TABLE I. Energy levels in Ne^{20}. Unless otherwise indicated, the entries are the results of the analysis of the elastic-scattering excitation curves, and the values are determined by inspection of the curves. Results from the elastic-scattering angular-distribution analyses and the inelastic-scattering experiment are labeled with the appropriate superscripts.

E_α (MeV)	Γ (keV,lab)	E_x (MeV)	J^π	E_α (MeV)	Γ (keV,lab)	E_x (MeV)	J^π
10.05	130	12.77	4^{+a}	13.58		15.59	
10.14	68	12.84		13.73		15.72	
10.32	75	12.99	(4^+)	14.05		15.97	
10.43	90	13.07	$(4^+)^b$	(14.53)		(16.35)	
10.57	75	13.19	(4^+)	14.69		16.48	
10.73	90	13.32	(4^+)	(14.91)		(16.66)	(1^-)
10.87	140	13.43	(4^+)	15.18	400	16.87	6^{+c}
11.20	400	13.69	$(3^-,7^-)$	15.73	340	17.32	$(2^+)^d$
11.51	125	13.94	(6^+)	16.01	230	17.54	
(11.77)		(14.148)		16.30	230	17.77	
11.97	300	14.30	6^{+a}	(16.53)		(17.95)	
(12.06)		(14.38)		16.70	180	18.09	(6^+)
12.31	300	14.58	(4^+)	16.98	300	18.32	(6^+)
12.66	150	14.86					
12.86	150	15.02		17.45		18.69	(6^+)
13.165	150	15.25		18.05	250	19.17	(6^+)
13.22		15.30		18.35	350	19.41	6^{+a}
13.37	470	15.43	7^{-a}	18.90	350	19.85	6^{+a}

a Levels with tentative spin and parity assignments confirmed by elastic-angular-distribution analysis.
b Consistent with the assignment from the inelastic-scattering experiment for a level $E_x = 13.04$ MeV.
c Assignment based on the elastic-angular-distribution analysis only.
d Spin and parity assignment from the inelastic-scattering experiment for a level at $E_x = 17.29$ MeV.

periment since only natural parity levels are detected in this experiment. Furthermore, a state which has a large α-particle width may have a very small proton width, and may be overlooked in an $F^{19}+p$ experiment.

From an inspection of the excitation curves, the group of levels between 10 and 11 MeV are all assigned a tentative spin-and-parity value of 4^+, except for the level at 10.14-MeV bombarding energy. This can be inferred from the absence of the anomalies in the excitation curves at the center-of-mass angle of 149.4°, a zero of $P_4(\cos\theta)$. The level at 10.14-MeV bombarding energy appears to be an odd spin and parity state.

Groups of levels such as the 4^+ levels between 10 and 11 MeV are expected if a single α-particle state is coupled with more complicated modes of excitation. No analysis of this possible intermediate structure was attempted in this work, but reference is made to a model which incorporates such effects in Sec. IV.

The resonance at 11.20-MeV incident energy does not show up at 90° and at 137.9°, which are zeros of all odd Legendre polynomials and that of order 7, respectively. Its effect at 140.8°, which is a zero of $P_3(\cos\theta)$, is also negligible. Thus the level at 13.69-MeV excitation in Ne^{20} is an odd spin-and-parity level, either a 3^- or a 7^- assignment would be consistent with this data.

Negligible effect of the resonance at 11.51 MeV is observed at 158.8°, a zero of $P_6(\cos\theta)$. The broad peak seen at that angle at about 11.3 MeV is probably due to the level discussed in the previous paragraph. Thus the level at 13.94 MeV in Ne^{20} corresponding to this resonance has been tentatively assigned a spin and parity of 6^+.

The next level to be considered is at 15.42-MeV excitation in Ne^{20} corresponding to the strong resonance at 13.37-MeV bombarding energy. This anomaly seems

to be composed of a number of resonances, and a careful examination reveals three components. They are at 13.16-, 13.37-, and 13.58-MeV bombarding energy, respectively. The resonance at 13.37 MeV has an experimental width of about 475 keV, and its effect at 90° and at 137.9° is very small. Consequently, this level is assigned a spin and parity of 7^-, which is confirmed by an angular-distribution analysis.

The resonance at α-particle energy 12.31 MeV vanishes at 149.4°, which suggests an assignment of 4^+ to the level at 14.58-MeV excitation in Ne^{20}.

The resonance at 14.91 MeV appears at all angles except 90°, where the rise to the next broad resonance is smooth and does not show any effect of this resonance. Although it is quite weak at the two most backward angles, it certainly does not vanish at those angles. Thus the probable assignment of the level at 16.66 MeV in Ne^{20} is 1^-.

Next, the group of resonances near the upper end of the excitation curves is considered. All of the last six resonances vanish at 158.8°, consequently the whole group of levels corresponding to these resonances may be assigned a spin and a parity of 6^+.

Hunt et al.[1] have shown that the Ne^{20} levels at excitation energies 12.77 13.69, 13.94, 14.3, and 15.43 MeV with assignments 4^+, (7^-), (6^+), 6^+, and 7^-, respectively, could be fitted into the rotational-band scheme proposed by Litherland et al.[19] An association of the several 6^+ levels at 16.87-MeV excitation energy and above with rotational bands has not been attempted because of insufficient information about possible lower-spin band members.

19 A. E. Litherland, J. A. Keuhner, H. E. Gove, M. A. Clark, and E. Almqvist, Phys. Rev. Letters 7, 98 (1961).

D. Analysis of the Angular Distributions

1. General Remarks

Dispersion theory may be used to calculate the theoretical angular distributions, but the practical limitation on the number of open channels and the level density precludes its application here. Hence the angular distributions measured in the present experiment are analyzed in terms of the APMB (Ackhiezer-Pomeranchuk-Blair-McIntyre) and the nuclear optical models. Resonant phase shifts are included in the APBM-model analysis where required to fit the data.

2. APBM-Model Analysis

In the APBM model, α-particle scattering is visualized in terms of a semiclassical boundary condition.[10] The fundamental assumption is that all particles that strike the nucleus are absorbed and that the rest are scattered by the Coulomb potential of the nucleus.

The expression[11] for the elastic-scattering cross section is

$$d\sigma/d\omega = |f(\theta)|^2,$$

and

$$f(\theta) = (2ik)^{-1} \sum_{l=0}^{\infty} (2l+1)(\eta_l - 1)P_l(\cos\theta), \qquad (1)$$

where $k = \hbar/(\mu v)$ with μ as reduced mass and v is the relative velocity.

In the APB model, conditions are imposed on η_l by the equations

$$\eta = 0 \qquad l \leqslant l'$$

and

$$\eta = \exp(2i\sigma_l) \qquad l > l',$$

where σ_l is the Coulomb phase shift and is given by

$$\sigma_l = \sigma_0 + \sum_{m=1}^{l} \tan^{-1}(\eta/m), \qquad \eta = ZZ'e^2/\hbar v.$$

By considering classical orbits, l' can be expressed as

$$\hbar^2 l'(l'+1) = 2\mu R^2 [E - (ZZ'e^2/R)],$$

where R is the sum of the radii of the target nucleus and the projectile, E is the energy, Z and Z' are the atomic numbers of target and the projectile, μ is the reduced mass and e is the electronic charge.

The sharp cutoff of η_l at $l = l'$ neglects barrier penetration and diffuseness. McIntyre[12] modified the APB model by introducing a smooth cut off for η_l in order to obtain better fits at backward angles. This modification consists of writing η_l as

$$\eta_l = A_l \exp[2i(\sigma_l + \delta_l)], \qquad (2)$$

where σ_l is the Coulomb phase shift, and δ_l is a nuclear phase shift. The quantities A_l and δ_l are expressed by the equations

$$A_l = \{1 + \exp[(l_A - l)/\Delta l_A]\}^{-1} \qquad (3)$$

and

$$\delta_l = \delta_0 \{1 + \exp[(l - l_\delta)/\Delta l_\delta]\}^{-1}. \qquad (4)$$

Thus in the APBM model a nuclear phase shift is also introduced. Substituting Eqs. (2), (3), and (4) in Eq. (1), the expression for the differential cross section for elastic scattering is given by

$$\frac{d\sigma}{d\omega} = (2k)^{-2} | \eta \sin^{-2}(\theta/2)e^{2i\sigma_0} \exp[-i\eta \ln(\sin^2(\theta/2))]$$

$$+ i \sum_{l=0}^{\infty} (2l+1)e^{2i\sigma_l}(A_l e^{2i\delta_l} - 1)P_l(\cos\theta) |^2.$$

If a particular angular distribution corresponds to an energy at which the excitation curves exhibit strong resonance behavior, the effects of the resonance on the angular distribution may be parameterized by a resonant nuclear phase shift. This procedure was used by Bromley et al.[20] in the analysis of the elastic scattering of C^{12} from C^{12}, and later by Carter et al.[21] in the study of α-particle scattering by C^{12}. An estimate of the δ_l value can be made from the behavior of the excitation curves at various angles.

If the reaction cross section is small at the resonant energy, then A_l for the l value characterizing the resonance is approximately equal to unity. For this situation, the magnitude of the Legendre-polynomial coefficients is maximized when the value of δ_l is $\pi/2$, which is chosen as the resonance condition. Large-reaction cross sections are manifest in small values of A_l. All other δ_l and A_l are determined by Eqs. (3) and (4) with the adjustable parameters l_A, Δl_A, δ_0, l_δ, and Δl_δ. These other δ_l may be considered as the background phase shifts and would serve the same purpose as the hard-sphere and other nonresonant phase shifts in the dispersion theory. In a comparison of the expression for differential cross section given above with the general expression given by partial-wave analysis, the δ_l are identified with the real part of the phase shifts of the partial waves and A_l is interpreted as $\exp(2i\delta_{lI})$ where δ_{lI} are the imaginary part of the partial-wave phase shifts.

A computer program written for an IBM 704 computer by Alster[22] was modified to include the provision for reading in the resonance phase shifts and the corresponding A_l. This modified program was used to obtain the theoretical angular distributions which are shown in Fig. 3. The parameters used to obtain the fits shown in Fig. 3 are listed in Table II, and the value of the nonresonant phase shift δ_l is zero unless otherwise specified in the table. If the value $\delta_l = \pi/2$ is associated with a resonance which is excited by the lth partial wave, then the level corresponding to the resonance can be assigned a spin $J = l$ and a parity $\pi = (-1)^J$.

[20] D. A. Bromley, J. A. Kuehner, and E. Almqvist, Chalk River Report No. PD-316, 1960 (unpublished).
[21] E. B. Carter, G. E. Mitchell, and R. H. Davis, Phys. Rev. **133**, B1421 (1964).
[22] J. Alster, University of California Reports No. UCRL-9650, No. UC-34, No. TID4500, 1961 (unpublished).

TABLE II. APBM parameters used in the theoretical fits of Fig. 3.

Curve	l_A	Δl_A	l	δ_l(rad)	A_l
1	4.0	1.0	2	2.4	0.6
			4	1.57	1.0
			5	2.3	0.8
2	4.0	1.0	2	2.5	0.5
			4	1.57	1.0
3	5.0	1.0	5	1.0	0.5
			6	1.57	0.75
4	5.0	0.5	7	1.57	1.0
5	6.0	1.5	6	1.57	1.0
			7	0.4	0.9
6	6.0	0.5	6	1.0	0.5
7	6.5	0.05	No other phase shift		
8	6.5	2.0	6	1.57	1.0
			7	2.2	0.3
			8	1.0	0.5
9	6.5	1.0	6	1.57	1.0
			7	2.2	0.3
			8	1.0	0.5

It is apparent from the excitation curves that there is hardly any region which is free from structure, and it was not possible to obtain a good APBM-model fit to the angular distributions without considering contributions from several resonances. A large number of parameters sets were tried. In the case of the angular distribution at 17.22 MeV a very small smoothing parameter Δl_A (which is equivalent to the sharp-cutoff Blair model) gave a fairly good initial fit with no resonance term added. This and the improvement made by adding an $l=6$ resonance term are both shown.

On examining the parameters given in Table II, it is seen that at 13.37-MeV bombarding energy only one value of δ_l, i.e., $\delta_7=1.57$ is required to fit the experimental data. Thus, the level at 15.43 MeV in Ne^{20} corresponding to this bombarding energy is a 7^- state. This state is already assigned as 7^- in Table I from the examination of the excitation curves.

In order to fit the other angular distributions, phase shifts for two or three partial waves had to be included. However, whenever a particular phase shift is close to $\frac{1}{2}\pi$, the level giving a major contribution to the angular distribution can be assigned a spin-and-parity value corresponding to the partial wave. On this basis the level at 12.77-MeV excitation corresponding to the bombarding energy of 10.05 MeV is assigned a spin and parity of 4^+, and contributions from 2^+ and 5^- levels are also present. The levels at 14.30, 16.87, 19.41, and 19.85 MeV in Ne^{20} corresponding to the bombarding energies of 11.97, 15.18, 18.35, and 18.9 MeV, respectively, are assigned a spin and parity of 6^+. Neighboring unidentified 7^- and 8^+ levels also effect the angular distributions at 18.35 and 18.9 MeV. A 5^- level influences the angular distribution at 11.97 MeV and a 7^- level the distribution at 15.18 MeV. The angular-distribution analysis confirmed five of the eighteen assignments made by inspection of the excitation curves. The assignment

for the resonance at incident energy 15.18 MeV is based on the angular-distribution analysis alone.

3. Optical-Model Analysis

In the nuclear optical model, the target nucleus is represented by a complex potential. The wave function of the target-projectile system is calculated by numerically solving the Schrödinger equation, and the complex phase shifts are calculated by imposing proper boundary conditions. This model was introduced to describe neutron-reaction cross sections[23] and was later applied to proton scattering,[24-26] α-particle scattering,[27-29] and heavy-ion scattering.[30,31]

An IBM 709 code made available by the Oak Ridge National Laboratory was used in this optical-model analysis. The complex potential used is of the form

$$V(r) = U_R\left[1+\exp\left(\frac{r-R_R}{a_R}\right)\right]^{-1}$$
$$+iW_{SI}\left[1+\exp\left(\frac{r-R_I}{a_I}\right)\right]^{-1}$$
$$+i4W_{DI}\exp\left(\frac{r-R_I}{a_I}\right)\left[1+\exp\left(\frac{r-R_I}{a_I}\right)\right]^{-2},$$

where U_R is the depth of the real part of the potential, W_{SI} is the volume term of the imaginary part of the potential, W_{DI} is the surface term, and a_R and a_I are diffuseness parameters for the real and imaginary potentials, respectively. The radius R is given by $R=r_0 \times(A^{1/3}+1.3)$, which is the form used by Igo.[28] A parameter R_{0R} is used in the program, where $R=R_{0R}A^{1/3}$.

In the present analysis the real radius and the imaginary radii were set equal, and the same condition held for the diffuseness parameters. The optical-model fits are shown in Fig. 4, and the parameters used to obtain the fits are listed in Table III. It can be seen that the fits are poor in comparison with the APBM fits with resonances. A limited-parameter search did not encourage a more exhaustive effort since the fits did not approach the agreement found with APBM-model analysis.

In order to obtain even qualitative agreement with

[23] H. Feshbach, C. E. Porter, and V. F. Weisskopf, Phys. Rev. 96, 448 (1954).
[24] A. E. Glassgold, W. B. Cheston, M. L. Stein, S. B. Schuldt, and G. W. Ericson, Phys. Rev. 106, 1207 (1957).
[25] A. E. Glassgold and P. J. Kellogg, Phys. Rev. 107, 1372 (1957).
[26] M. A. Melkanoff, J. S. Nodvik, D. S. Saxon, and R. D. Woods, Phys. Rev. 106, 793 (1957).
[27] W. B. Cheston and A. E. Glassgold, Phys. Rev. 106, 1215 (1957).
[28] G. Igo and R. M. Thaler, Phys. Rev. 106, 126 (1957).
[29] G. Igo, Phys. Rev. 115, 1665 (1959).
[30] C. E. Porter, Phys. Rev. 99, 1400 (1955).
[31] R. H. Bassel and R. M. Drisko, in Proceedings of the International Conference on Nuclear Structure, Kingston, Canada, edited by D. A. Bromley and E. W. Vogt (University of Toronto Press, Toronto, 1960), p. 212.

TABLE III. Optical-model parameters used in theoretical fits of Fig. 4.

Curve No.	U_R (MeV)	R_{OR} (F)	a_R (F)	W_{SI} (MeV)	W_{DI} (MeV)	r_0 (F)
1	150	1.93	0.5	...	3	1.40
3	150	1.93	0.5	...	3.0	1.40
2	150	1.87	0.5	...	3.0	1.35
5	150	1.97	0.5	...	5.0	1.45
4	150	1.97	0.5	...	3.0	1.45
6	150	1.87	0.5	...	5.0	1.35
7	135	1.87	0.5	...	5.0	1.35
9	150	1.93	0.5	...	7.5	1.40
8	125	1.93	0.5	5.0	...	1.40
10	75	2.12	0.5	...	3.0	1.60
11	125	1.97	0.5	...	5.0	1.45
12	75	2.12	0.5	...	3.0	1.60
13	125	1.97	0.5	...	5.0	1.45

the experimental results, rather large real potentials (about 150 MeV) were required in the optical-model calculations below 18-MeV bombarding energy. Above 18 MeV, a real potential of 75 MeV was used. Otherwise, there were no large changes in the values of the parameters at different energies. Most of the fits were obtained with surface imaginary potentials, except at 17.22 MeV, where a better fit was obtained with a volume imaginary potential. In general, the imaginary potentials were between 3 and 5 MeV.

This failure of the optical model to reproduce the experimental angular distributions is not surprising. The optical model predicts only the average cross sections and does not take into account any compound nuclear resonances individually. These are couched in the imaginary part of the potential. If specific resonance contributions are included in the optical-model computation, as is done in the APBM calculations, better fits to the experimental data may be obtained.[32]

A possible extension of the optical model is to analyze the elastic as well as the inelastic-scattering data by using coupled Schrödinger equations. This is discussed by Mitchell et al.[33] in the analysis of inelastic scattering of α particles by C^{12}. In the present case a coupled-equations analysis is not possible, since the angular distributions of the inelastically scattered α particles were not measured.

III. γ-RAY EXPERIMENT

A. Experimental Technique

The yield of γ rays produced by the α-particle bombardment of O^{16} were measured at $0°$ as a function of α-particle energy. The α-particle beam, collimated by a tantalum collimator with a 0.5-in. hole, impinged on the target, which was made by depositing lead oxide on 0.005-in.-thick gold disks 1.5 in. in diameter. γ rays emitted by the target in a forward cone of half-angle of

[32] G. E. Brown, in *Proceedings of the International Conference on Nuclear Structure*, edited by D. A. Bromely and E. W. Vogt (University of Toronto Press, Toronto, 1960), p. 135.

[33] G. E. Mitchell, E. B. Carter, and R. H. Davis, Phys. Rev. **133**, B1434 (1964).
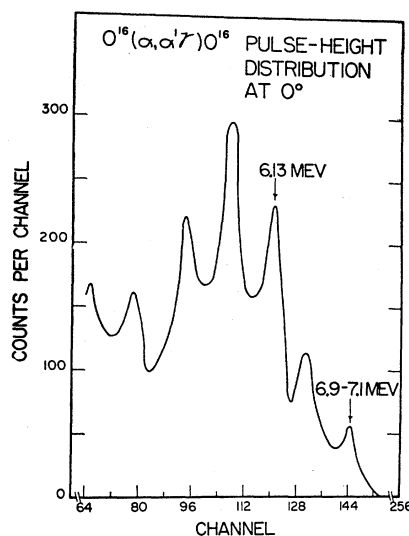

FIG. 5. Typical pulse-height spectrum for γ rays from the $O^{16}(\alpha,\alpha'\gamma)O^{16}$ reaction. The 6.13-MeV γ ray and the 6.92–7.12-MeV unresolved γ rays are shown.

about $37°$ were detected by a 3-in.$\times$3-in. NaI(Tl) crystal and photomultiplier unit, obtained from Harshaw Chemical Company, placed at a distance of 2 in. from the target. Signals from the preamplifier were fed into a TMC 256-channel analyzer after proper amplification. Figure 5 shows a typical pulse-height distribution for the 6.13-MeV and unresolved 6.92- and 7.12-MeV γ rays produced by the decay of the second, third, and fourth excited states.

For the angular-distribution measurements, the targets were mounted in a thin walled chamber. A 3-in. $\times$3-in. NaI(Tl) crystal was mounted on a rotating arm at a distance of 10 in. from the axis of rotation and subtended an angle of about $17°$. Steps in angle were $15°$. Another 3-in.$\times$3-in. NaI(Tl) crystal was placed at fixed angle of $90°$ with respect to the beam and served as a monitor.

To determine the target thickness, the elastic-scattering yield from the same target was measured and compared with the elastic cross section known from the previous experiment. The peak-to-total ratio and the efficiency of the crystal for the detection of 6-MeV γ rays were estimated by extrapolating the known curves for the 3-in.$\times$3-in. NaI(Tl) crystal.[34] The error in the absolute cross section for the 6.13-MeV γ-ray excitation curve is estimated to be about $\pm45\%$. The cross section for the 7-MeV γ ray is lower than that for the 6.13-MeV γ ray by a factor of approximately 5. The two excitation curves are shown in Fig. 6.

Although the excitation curve revealed some well-resolved resonances, the resonances overlapped to a large extent. There are only two cases where the resonances stand out prominently above the background.

[34] R. L. Heath, U. S. Atomic Energy Commission Report No. IDO-16408, 1957 (unpublished).
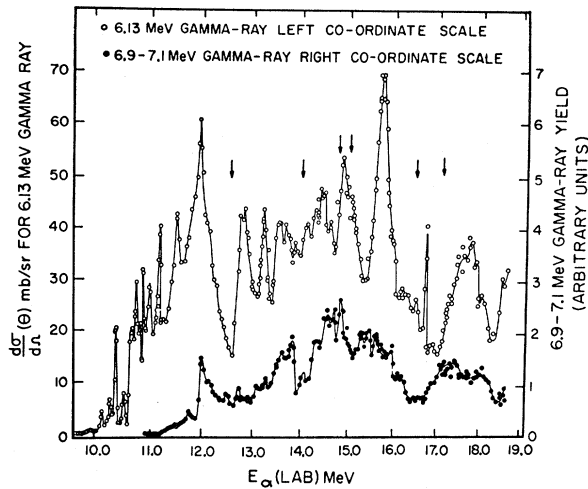
FIG. 6. Excitation functions for the 6.13-MeV and the unresolved 6.92–7.12-MeV γ rays from the $O^{16}(\alpha,\alpha'\gamma)O^{16}$ reaction. The left scale is for the 6.13-MeV γ rays, and the right one is for the higher-energy γ rays.

These are the resonances at 10.39 and 15.705 MeV, where the ratio of the cross section on the peak to that in the valley is about 10 and 3, respectively. Angular distributions using thin targets (about 25 keV thick for 10-MeV α particles) were measured at several energies which straddled these peaks, and the results are shown in Fig. 7. In order to study the gross structure effects, angular distributions were also measured with considerably thicker targets (about 250 keV for 10-MeV α particles) at six energies distributed throughout the energy range. These are shown in Fig. 8. All the angular distributions in Figs. 7 and 8 were found to be symmetric about 90°.

Important information may be obtained from an angular distribution without a precise value for the absolute cross section. Each angular distribution was assumed to have the following form:

$$\frac{W(\theta)}{W(90°)} = A_0 P_0(\cos\theta) + A_2 P_2(\cos\theta)$$
$$+ A_4 P_4(\cos\theta) + A_6 P_6(\cos\theta), \quad (5)$$

where $W(\theta)$ is the yield at any angle. $W(90°)$ is the yield at 90°; A_0, A_2, A_4, and A_6 are constants, and the P_l are the Legendre polynomials. An IBM 709 computer was programmed to make a least-squares fit of the data for each angular distribution to the above expression and extract the values of the relative coefficients A_2/A_0, A_4/A_0, and A_6/A_0. These are listed in Table IV. The estimated relative error in these values is $\pm15\%$.

B. Analysis of the Excitation Curves

Each of the excitation curves exhibits a considerable amount of structure. With few exceptions, resonances are seen in both curves. For example, the prominent resonance at 15.705 MeV in the 6.13-MeV γ-ray curve

shows up very weakly in the $\sim$7-MeV γ-ray curve. The rise in the average cross section beyond 11 MeV for the higher-energy γ-ray curve and beyond 10 MeV for the 6.13-MeV γ-ray curve is due to the penetration of the Coulomb barrier by the outgoing α particles.

The levels in Ne[20] corresponding to peaks in the excitation curves are listed in Tables V and VI. Estimates of the observed widths are also listed. These can be compared with the levels listed in Table I. As discussed earlier, the excitation energy values in Table I are uncertain by as much as the observed widths. Taking this into consideration, the correspondence between the two sets is good, but there are a few cases where a particular level is seen in the elastic excitation curve and does not show up in the γ-ray data and vice versa. These occur
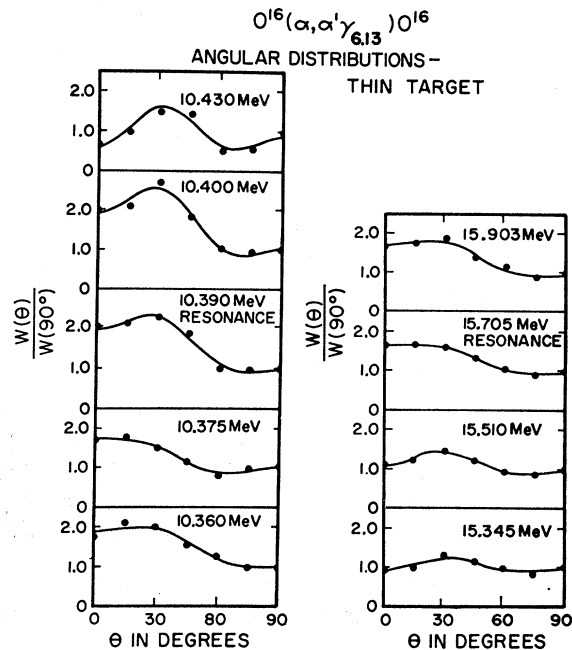
TABLE IV. Coefficients extracted from a least-squares fit to 6.13-MeV γ-ray angular distribution.

	E_α (MeV)	A_2/A_0	A_4/A_0	A_6/A_0
1	10.360	0.629	−0.040	−0.207
2	10.375	0.483	0.310	−0.228
3	10.390	0.809	−0.001	−0.394
4	10.400	0.900	−0.024	−0.559
5	10.430	0.588	−0.063	−0.895
6	15.345	0.208	−0.095	−0.249
7	15.510	0.375	−0.019	−0.351
8	15.705	0.480	−0.070	−0.164
9	15.903	0.579	−0.004	−0.236
10	12.66	0.588	−0.228	−0.437
11	13.995	0.483	−0.075	−0.266
12	14.745	0.474	0.080	−0.596
13	14.960	0.549	0.027	−0.402
14	16.410	0.324	−0.116	−0.026
15	17.105	0.104	−0.100	−0.188

FIG. 7. Angular distributions of the 6.13-MeV γ rays obtained with a thin (about 25 keV for 10-MeV α particles) target.

TABLE V. Energy levels in Ne²⁰ observed in the 6.13-MeV γ-ray excitation curve.

E_α (MeV)	E_x (MeV)	Γ (keV,lab)	E_α (MeV)	E_x (MeV)	Γ (keV,lab)
10.14	12.84	70	15.50	15.53	
10.275	12.95	40	13.63	15.63	
10.39	13.04	40	13.84	15.80	
10.53	13.15	70	14.08	15.99	
10.69	13.28	100	14.26	16.14	
10.76	13.33	100	14.37	16.23	
10.83	13.39	50	14.45	16.29	
10.87	13.43	70	14.55	16.37	
11.00	13.53	200	14.83	16.59	
11.18	13.67	50	15.705	17.29	400
11.49	13.92	200	16.16	17.65	
11.92	14.26	300	16.47	17.91	
12.71	14.90		16.70	18.09	
12.80	14.97		16.84	18.20	
13.19	15.28		17.600	18.81	750

TABLE VI. Energy levels in Ne²⁰ observed in the 6.9–7.1-MeV γ-ray excitation curve.

E_α (MeV)	E_x (MeV)	E_α (MeV)	E_x (MeV)
11.73	14.11	14.53	15.97
11.97	14.30	14.66	16.46
12.11	14.42	14.80	16.57
12.46	14.70	15.290	16.96
12.71	14.90	15.434	17.08
12.84	15.00	15.60	17.21
13.31	15.34	15.96	17.50
13.58	15.59	16.13	17.63
13.79	15.76	17.22	18.51
14.05	15.97	18.05	19.17
14.26	16.14		

where the width of the elastic-scattering anomaly is large.

C. Analysis of Angular Distributions

Kraus et al.[35] have given an expression for the angular distributions of nuclear reactions of the type $(a,b\gamma)$. In the present case the 6.13-MeV γ ray is emitted from a 3⁻ state. If a pure compound-nucleus level is assumed, the expression for the angular distribution takes the form

$$\sigma(\theta)=\sum_{l'\Delta} \pi\lambda_a^2 S^2(sls'l',J\pi)|\langle 0\|H(3)\|3\rangle|^2(-2)i^{-\Delta}(-1)^{l'}$$

$$\times[(2J+1)49]C(331-1,\,\Delta 0)Z(JJJJ,0\Delta)$$

$$\times W(J3J3,l'\Delta)W^2(3333,0\Delta)P_\Delta(\cos\theta).$$

The symbols have the following meanings: J is the spin of the compound-nuclear state, l is the relative angular momentum in the incoming channel, s is the incoming channel spin, which is zero, and $l=J$, l' is the relative angular momentum in the outgoing channel, s' is the outgoing channel spin which is 3, and l' is limited by $|J-3|<l'<J+3$. The quantity $S(sls'l',J\pi)$ is the ap-

[35] A. A. Kraus, Jr., J. P. Schiffer, F. W. Prosser, Jr., and L. C. Biedenharn, Phys. Rev. 104, 1667 (1956).

O¹⁶(α,α'γ₆,₁₃)O¹⁶
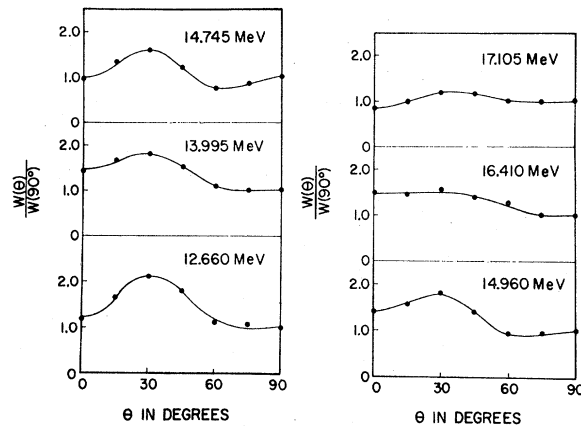ANGULAR DISTRIBUTIONS-THICK TARGET

FIG. 8. Angular distributions of the 6.13-MeV γ ray obtained with a thick (about 250 keV for 10-MeV α particles) target.

propriate element of the scattering matrix, $\langle 0\|H(3)\|3\rangle$ is the γ-ray-transition matrix element, Δ is a dummy-summation index and is even (if the transition is assumed to be pure E3). Since the angular distribution of a γ ray of multipolarity L cannot have terms with Legendre polynomials of orders higher than $2L$, the higest value of Δ is 6.[35] The rest of the symbols are the reduced wavelength of the bombarding particle, the Racah coefficients Z and W,[36] and the Clebsch-Gordan[37] coefficients C.

For a given value of J^π, more than one value of l' may contribute. These contributions add incoherently; hence the contribution from each l' may be calculated separately and the results linearly combined.

For a given J all the quantities that do not depend on either l' or Δ are constants and can be collected into one. The coefficients $W^2(3333,0\Delta)$ are the same for all values of Δ, and can be absorbed into the general constant. Thus for a given value of J and one of the possible values of l', the cross section can be written as

$$\sigma(\theta)=\text{const}\times\sum_\Delta (-1)^{l'}C(331-1,\,\Delta 0)Z(JJJJ,0\Delta)$$

$$\times W(J3J3,l'\Delta)P_\Delta(\cos\theta).$$

Writing this in the form of Eq. (5), the relative coefficients A_2/A_0, A_4/A_0, and A_6/A_0 can be expressed in terms of the Racah coefficients and can be calculated. This treatment assumes a point geometry, and a correction for finite geometry should be applied to the theoretical values.[38] Table VII lists the corrected theoretical relative coefficients for values of J from 0 through 7 and all possible l' values for each J.

[36] L. C. Biedenharn, J. M. Blatt, and M. E. Rose, Rev. Mod. Phys. 24, 249 (1952).
[37] E. U. Condon and G. H. Shortly, Theory of Atomic Spectra (Cambridge University Press, Cambridge, England, 1935).
[38] A. M. Feingold and S. Frankel, Phys. Rev. 97, 1025 (1955).

TABLE VII. Theoretical angular-distribution coefficients for the 6.13-MeV γ ray. Finite-geometry corrections are included.

J	l'	A_2/A_0	A_4/A_0	A_6/A_0
1	2	0.592	0	0
1	4	0.248	0	0
2	1	0.847	0.133	0
2	3	−0.386	0.133	0
2	5	0.352	0.007	0
3	0	0.985	0.259	−0.225
3	2	0.310	−0.126	−0.776
3	4	−0.490	0.133	−0.095
3	6	−0.414	0	0
4	1	0.882	0.166	−0.509
4	3	0.097	−0.464	−0.837
4	5	−0.517	−0.119	−0.201
5	2	0.820	0.80	−0.271
5	4	−0.021	−0.099	−0.761
5	6	−0.502	0.099	−0.831
6	3	1.095	0.113	−0.183
6	5	−0.090	−0.080	−0.755
6	7	0.495	0.093	−0.246
7	4	0.764	0.013	−0.145
7	6	−0.138	−0.007	−0.705
7	8	−0.490	0.106	−0.271

TABLE VIII. Comparison of the 6.13-MeV γ-ray angular-distribution coefficients measured at incident energy 10.39 MeV with the theoretical values. A pure state is assumed in the calculations.

Theoretical \ Experimental		A_2/A_0 0.809	A_4/A_0 −0.001	A_6/A_0 −0.394
J	l'			
4	1	0.882	0.166	−0.509
4	All l'	0.802	0.102	−0.590
5	2	0.820	0.08	−0.271
5	All l'	0.742	0.068	−0.322

Before comparing the relative coefficients given in Table VII with those experimentally measured, an additional assumption is necessary to determine the relative weights of the contributions of the several l' values for a given J value. A linear combination may be formed by weighting the contributions from all possible l' for a given J with the penetrabilities of the outgoing partial waves. If it is assumed that the elements $S(sls'l'; J^{\pi})$ depend on l' through the kinematic factor $k'r/(F_{l'}{}^2,G_{l'}{}^2)$ only, the square of the scattering matrix element is given by

$$[S(l')]^2 = [k'r/(F_{l'}{}^2 + G_{l'}{}^2)](S')^2,$$

where k' is the wave number in the outgoing channel, r is the interaction radius, and $F_{l'}$ and $G_{l'}$ are the Coulomb wave functions. For a particular energy and a chosen J, the quantities S', k, and r are constants. The penetrability $1/A_{l'}{}^2 = 1/(F_{l'}{}^2 + G_{l'}{}^2)$ is a function of $k'r$ and η', with η' given by

$$\eta' = 0.157 Z Z' \left\{ \frac{mm'/(m+m')}{[m/(m+m')]E+Q} \right\}^{-1/2},$$

and it refers to the outgoing channel.[39]

The experimental values of the relative coefficients for the resonance at incident energy 10.39 MeV are compared with the theoretical values for $J=4$ and $J=5$ in Table VIII. Theoretical coefficients for a single l' and penetrability weighted values for all l' are shown. The theoretical fits for these cases are shown in Fig. 9 where the points are experimental values and the lines are the theoretical fits. A spin-and-parity assignment of either 4^+ or possibly 5^- to the state at 13.04 MeV in the Ne²⁰ corresponding to the E_α of 10.39 MeV is consistent with the γ-ray angular distribution. This is presumably the same state as the one identified at 13.07 MeV in the

elastic-scattering experiment which is tentatively assigned a spin and parity of 4^+.

The resonance at 15.705 MeV is apparently not due to a pure state, however, the major contribution may be from a single level. Assuming that the contribution from all the interfering neighbors is incoherent and constitutes a background, a background correction was made by subtracting the yield just off the resonance. The relative coefficients extracted after the angular distribution at 15.345 MeV is subtracted from the one at 15.705 MeV are shown in Table IX, together with the theoretical values that are in closest agreement. A strong preference for $J=2$ and $l'=1$ is indicated as shown in Fig. 9. The experimental points are plotted after the background subtraction. It should be noted that a penetrability weighted linear combination of the contributions from all l' for $J=2$ gives relative coefficients that are very different from the experimental values. Moreover, there is no set of values listed in Table VII which is close to the experimental values for the angular distribution at 15.705 MeV without the background subtraction.

A spin-and-parity assignment of 2^+ is given to the resonance at incident energy 15.705 MeV ($E_x = 17.29$ MeV). The state closest to this one observed in the elastic-scattering data is at 17.230, but a spin-and-parity assignment is not possible in that experiment.

[39] W. T. Sharp, H. E. Gove, and E. B. Paul, Atomic Energy Commission Limited Report No. 268, 1960 (unpublished).

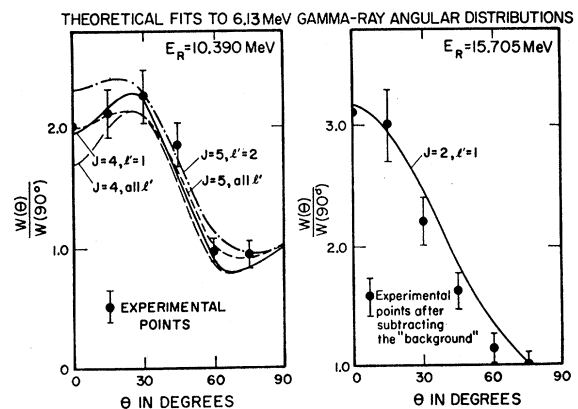THEORETICAL FITS TO 6.13 MeV GAMMA-RAY ANGULAR DISTRIBUTIONS

FIG. 9. Theoretical fits to the angular distribution at 10.390 MeV and at 15.705 MeV. The dots are the experimental values, and the lines are the theoretical fits. The symbols J and l' are discussed in the text and are listed in Tables VIII and IX.

TABLE IX. Comparison of the 6.13-MeV γ-ray angular-distribution coefficients measured at 15.705-MeV bombarding energy with theoretical values. A background has been subtracted from the experimental distribution, and a pure state is assumed in the calculations.

		A_2/A_0	A_4/A_0	A_6/A_0
Experimental (background subtracted)		0.881	0.321	0.018
Theoretical				
$J=2$	$l'=1$	0.847	0.133	0
$J=2$	all l'	0.377	0.116	0

Thick-target (250 keV thick to 10-MeV α particles) angular distributions were measured at the energies indicated by the arrows in Fig. 6 and are shown in Fig. 8. If the target is sufficiently thick, the yield represents an average over a large number of sharp resonances and the interference effects of these resonances may cancel out, and gross structure effects may be apparent.

The excitation curves suggest the existence of a wide resonance in the vicinity of 15 MeV. The angular distributions at 14.745 MeV and at 14.960 MeV are very similar, while the two on each side of these are different. If there is a nuclear state with a spin and parity of J^π corresponding to a wide resonance, and if the target is sufficiently thick to average over the narrow resonances, the angular distribution on the peak of the resonance would be given by the relative coefficients corresponding to the J value of the level. A comparison of the values given in Table VII with the experimental results yield no agreement for J values from 1 through 7. A penetrability weighted linear combination for all l' led to no improvement. No attempt was made to develop a model which would guide a further analysis of these results.

IV. DISCUSSION

The Ne^{20} excitation-energy range 12.72 to 19.93 MeV has been studied by means of several reactions, most of which are proton induced, and a large number of levels have been reported.[17,18] The number of energy levels in Ne^{20} listed in Table I is significantly smaller than that of the tabulation (Table 20.6) of Ref. 16. While a number of the excitation-energy values agree within the experimental error, the estimated widths in Table I are generally larger, and the spin assignments often disagree when a comparison can be made. The angular momenta measured in the α-particle scattering experiment are larger than those found in the studies of other reactions involving lighter projectiles. It appears that a somewhat different set of levels in Ne^{20} is preferentially observed in the scattering of α particles by O^{16} than is found in proton-induced reactions which form the same compound system.

Relative to the proton and deuteron channels leading to Ne^{20} at a given excitation energy, larger angular momenta are delivered via the α-particle channel, and because of the $(2l+1)$ dependence of the scattering am-

plitude (Eq. 1), higher partial waves may override the effects of lower-order partial waves. If low-orbital angular-momentum α particles are "absorbed" which is the case in the APBM model, the dominance of the large angular-momentum partial waves in the elastic scattering is increased.

Resonance terms were added to the APBM model to fit the angular distributions. This was necessary because of the structure in the excitation curves and these resonance terms provided information about the levels in Ne^{20}. One feature of the observed levels which deserves comment is the apparent grouping of states with the same spin-and-parity assignments. This may represent a distribution of single-particle strength among several compound-system or intermediate states. The coupling of compound-system states with single-particle (or potential) resonances can produce such behavior.[40]

Large values of the real potentials were used to obtain even qualitative fits with the nuclear optical model. No resonance terms were added in the optical-model analyses performed here, but this type of analysis may be important when more detailed data becomes available.

Excitation curves for the γ rays following the inelastic-scattering events confirmed the existence, within experimental errors in excitation energy, of most of the levels already identified in the elastic-scattering experiment, and two assignments have been made. Some giant-resonance phenomenon is suggested by the excitation curves, but attempts to interpret thick-target angular distributions in this fashion were unsuccessful. The negative result of this analysis could be due to the fact that only pure levels were assumed in the theoretical calculations, or that some direct process may dominate the interaction.

The most detailed comparison with previous results is possible in connection with the rotational bands in Ne^{20}, and certain results of this paper are included in the discussion of the rotational bands which is presented in Paper I.[1]

[40] R. H. Davis, in *Proceedings of the Symposium on Recent Progress in Nuclear Physics with Tandems*, edited by W. Hering (Max Planck Institute for Nuclear Physics, Heidelberg, 1966).